RSC Advances

ROYAL SOCIETY OF CHEMISTRY

www.rsc.org/advances

Journal Name

RSCPublishing

ARTICLE

Pulse reverse electrodeposition and characterization of nanocrystalline zinc coatings

Cite this: DOI: 10.1039/x0xx00000x

Qingyang Li, Zhongbao Feng, Jinqiu Zhang, Peixia Yang, Fenghuan Li and Maozhong An*

Received 00th January 2012,
Accepted 00th January 2012

DOI: 10.1039/x0xx00000x

www.rsc.org/

Nanocrystalline zinc coatings are produced through pulse reverse electrodeposition in acid sulfate electrolyte with polyacrylamide (PAM) as the only additive and characterized by field-emission scanning electron microscope (FESEM), atomic force microscope (AFM), transmission electron microscopy (TEM), X-ray diffraction (XRD) and energy dispersive X-ray spectroscopy (EDS). The influences of additive and electrodeposition parameters on the surface morphology, grain size and crystallographic preferred orientation of coatings are investigated. Mechanical, wear and corrosion resistance properties of nanocrystalline and coarse-grained zinc coatings are also evaluated by nanoindentation, ball-on-disc tribometer and immersion test, respectively. The results show that changing the electrodeposition parameters cannot produce nanocrystalline zinc coating in the absence of additive, and the PAM plays a crucial role in reducing the grain size of coating from micro to nano scale. The grain size of coating decreases asymptotically with increased forward pulse current density in the presence of PAM, and the pulse reverse current makes the coating smoother. Hardness of the nanocrystalline zinc coating (31 nm) is almost three times than that of the coarse-grained counterpart. Wear and corrosion resistance properties of nanocrystalline zinc coating are superior to coarse-grained counterpart.

Introduction

Zinc is anodic coating relative to carbon steel, iron and low alloy steel, which can play a role in electrochemical protection when it forms a micro-corrosion battery with steel based metal and the damaged area of coating surface is not too big. Moreover, the zinc coating is stable in air and it forms a layer of dense alkaline zinc carbonate film which plays a role in physical protection to the substrate in humid environment. Moreover, the low cost and easy application of zinc also make the electrodeposition of zinc coating become a major surface protection techniques and widespread application in protecting of steel against corrosion. As mentioned above, the success of using zinc as a steel coating can be attributed to its sacrificial nature, but the zinc coating does not alter the mechanical properties of the underlying base metal, and thereby the coating must be thick enough to endure attack of a corrosive environment. Thus, the poor mechanical properties of the conventional coarse-grained zinc coating have hindered its application in many fields. This provides the need to develop thinner electrodeposited coatings with improved properties such as hardness, corrosion, friction and wear, etc.[1-3]

Nanocrystalline electrodeposits have exhibited many unusual mechanical, physical, chemical and electrochemical properties due to its grain size below 100nm and high-volume fraction of the grain boundary.[4] The further researches have demonstrated that the nanocrystalline coatings possess excellent wear resistance,[5,6] corrosion resistance,[7,8] ductility,[9,10] hardness[11,12] and electrochemical properties[13] compared with conventional coarse-grained zinc coatings. Therefore, it is of great significance to improve the properties of conventional zinc coating through nano-electrodeposition technology.

So far, several nanocrystalline zinc coatings were obtained from various galvanizing bath, such as alkali,[14] chloride,[15] sulfate,[16] acetate[17] or citrate[18] system. Among these baths, sulfate bath has high current efficiency, less energy consumption, solution stability, simple maintenance characteristics, which can be used in high speed plating. Yan et al.[19] produced the nanocrystalline zinc coatings with laminated structure through direct current electrodeposition from sulfate bath, but it only achieved nanoscale in thickness direction not

in three dimensions grain size. Li M C et al.[20] obtained the nanocrystalline zinc coatings from sulfate bath containing the mixtures of thiourea and benzalacetone by pulse electrodeposition, with average grain sizes in the range of 60 to 77nm. The results show that it was not effective enough to induce the formation of nanocrystalline zinc in single addition or additive-free system. Gomes[21] also investigated the electrochemistry behaviors of electrodeposition of nanocrystalline zinc coatings in sulfate bath with cetyl trimethyl ammonium bromide (CTAB), sodium dodecyl sulphate (SDS) and octylphenolpoly(ethyleneglycolether)$_n$, n= 10, (Triton X-100) as surfactants and obtained the needle shape zinc coating with average grain sizes in the range of 20 to 40nm. It is also proved that the additive plays a crucial role in the process of grain refinement.

The current modes also have a significant effect on the surface nanocrystallization of coatings in the presence of additives. The most commonly used current modes in electrodeposition of zinc coatings include direct current, pulse current and pulse reverse current. Among these techniques, the pulse electrodeposition (or single pulse electrodeposition) had significant advantages in the control of grain size, surface morphology and preferred orientation of coating than direct current electrodeposition.[22] Compared with the pulse electrodeposition, the pulse reverse electrodeposition (or double pulse electrodeposition)[23-26] can significantly improve the thickness distribution, eliminate hydrogen embrittlement and remain the surface of coating in an activated state, so as to prepare smoother, denser, lower porosity and better adhesion coatings. Moreover, the anodic dissolution effect of pulse reverse current was beneficial to reduce the actual thickness of the diffusion layer and improve the cathodic current efficiency, further speed up the deposition rate of coating as well. Therefore, the zinc coatings produced by pulse reverse electrodeposition had better corrosion resistance than the coatings prepared through pulse electrodeposition[27], which fabricated the similar coatings in the bath without additives to the bright coatings prepared by direct current electrodeposition in the bath with additives.

So far, most research works have focused on the pulse electrodeposition of nanocrystalline zinc coatings and the electrochemical corrosion behaviour of the coatings.[2,3,14,18] There is rare study on the pulse reverse electrodeposition of nanocrystalline zinc coatings and the mechanical properties of the coatings. In this study, we produce nanocrystalline zinc coatings through combining the advantages of additive and pulse reverse current, and investigate their effect on surface topography, crystallographic preferred orientation and grain size of the coatings. Specially, the interests are focused on the different hardness, corrosion and tribological behavior between nanocrystalline zinc coating and conventional coarse-grained zinc coating.

Experimental

Electrodeposition of nanocrystalline zinc coatings

Zinc electrodeposition was carried out in a two-electrode cell containing 200 mL sulfate bath. The used substrates which were copper sheets of 4×4 cm^2 area were pretreated by immersion in a solution of 10% (volume ratio) hydrochloric acid at room temperature for 10s, and rinsed with distilled water. Zinc plate of 99.99% purity was used as anode. The sulfate bath was prepared by dissolving 100 g/L of $ZnSO_4$•$7H_2O$ and 20 g/L of H_3BO_3 in deionized water. Once dissolved, the pH value of the solution was adjusted to 1~2 with the addition of dilute sulphuric acid, followed by the addition of 1 g/L of nonionic type polyacrylamide (PAM MW=2000000) as grain refiner. The bath was heated under stirring until the PAM was fully dissolved and the electrolyte became transparent to complete the configuration process of bath. All solutions were prepared in AR grade chemicals and deionized water.

Pulse reverse electrodeposition or double pulse electrodeposition (The periodic reverse pulse current with pulse in both positive and negative direction.) was conducted by varying the pulse forward current density (J_f) from 1 to 4 A/dm^2 and the pulse reverse current density (J_r) from 0 to 0.5 A/dm^2. In order to study the influence of the reverse current density on surface topography, crystallographic preferred orientation and grain size of zinc coatings, the current-on time (T_{on}) and current-off time (T_{off}) were set to fixed values of 0.2ms and 0.8ms, respectively. And the electrodeposition time was 60min in a magnetically stirred system at room temperature, for all experiments.

The efficiency of current electrodeposition (η) was calculated by the Faraday's law according to equation (1). The amount of mass deposited in theory was compared with that of actual zinc mass deposited in the same current density and time.

$$\eta = \frac{m_2 - m_1}{I \cdot t \cdot K} \times 100\% \quad (1)$$

Where m_1 is the measured weight before electrodeposition (in g), m_2 is the weight after electrodeposition (in g), I is the current that flows through the cathode (in A), t is the time that the current flows (in h) and K is the electrochemical equivalent of Zinc (in 1.22 g/(Ah)).

Grain size characterization of coatings

A field-emission scanning electron microscope (FESEM, Helios Nanolab 600i) with energy dispersive X-ray spectroscopy (EDS) was used to examine the surface and cross-section morphology, grain size and the component of coatings. The grain size distribution of coatings was investigated by Nano Measure software, which was determined by measuring more than 100 points in FESEM image randomly to avoid feature point close clustering. Then the average grain size of coatings was obtained through Gaussian fitting for the measure results. Surface roughness was characterized by atomic force microscope (AFM, Bruker Multimode 8) working in the intermittent contact mode. X-ray diffraction (XRD, Rigaku Corporation Dmax-3B) was carried out using Cu Ka radiation for determining the crystallographic texture, crystallographic preferred orientation and approximate average grain size of coating. The grain size of coatings was calculated using the Scherrer's formula. Moreover, considering the sensitivity limitation of FESEM and the calculation error of XRD in grain size of coating, the transmission electron microscopy (TEM, JEM-2100) was performed for determining the grain size of coating obtained from optimum bath. Samples of nanocrystalline zinc coating were removed from the substrate using a sapphire knife without destroying the substrate, then dispersed in acetone. A drop of the solution was placed on the carbon-coated grid and inserted into the TEM. In any testing program, three times replicates should be included to certify the reproducibility.

Properties evaluation of coatings

Mechanical performance: Hardness values of the specimens were evaluated based on load-depth curves obtained by the nanoindentation tests (nanoindenter XP, MTS Systems Corporation). All measurements were made 1 μm penetration depth with a Berkovich diamond indenter. Typically, 5 indents were obtained for individual specimens, from which average values were calculated.

Friction and wear property: The friction coefficients of coatings were tested on ball-on-disk tribometer (Center for Tribology, HIT, China) with a 52100 steel ball of 10 mm diameter as friction partner. All experiments were performed under a load of 1 N and a sliding speed of 0.188 m/s without lubrication, at room temperature with a relative humidity of approximately 40%. The friction coefficient curves were recorded continuously during the test process.

Corrosion behaviour: The corrosion resistance property of samples is evaluated by immersion test, and the 3.5% NaCl solution (room temperature and closed environment) was used as corrosive medium. After the corrosion tests, the surface morphology and element composition of corrosion products were analysed by FESEM and EDS.

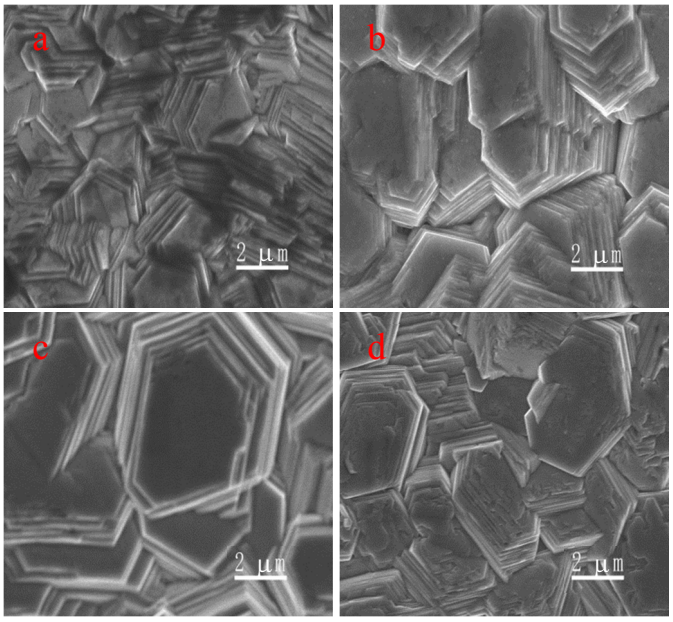

Fig. 1 Effect of J_f on the surface morphology of zinc electrodeposited from sulphate bath without additives: (a) 1 A/dm^2, (b) 3 A/dm^2, (c) 5 A/dm^2, and (d) 7 A/dm^2.

Results and discussion

Effect of pulse current density on grain size

In order to determine whether the change of J_f reflects the surface morphology or not, a SEM study is performed, as shown in Fig. 1. These SEM micrographs are obtained at J_f of 1, 3, 5 and 7 A/dm^2. The SEM images show that the surface morphology and grain size are markedly affected by the pulse current density. In the basic zinc sulphate bath (additive-free sulphate bath), the situation that the coatings display the hexagonal zinc plates aligned parallel to the substrate indicates that the hexagonal structure of zinc is preserved in the zinc electrodeposition. By comparing the coatings at different values of J_f from additive-free bath, it is found that the grain size increased gradually with increasing J_f. This result indicates that changing the electrodeposition parameters cannot produce nanocrystalline zinc, and the nucleation rate is lower than the growth rate of coatings in the absence of additives. The smallest grain size is produced at J_f=1 A/dm^2.

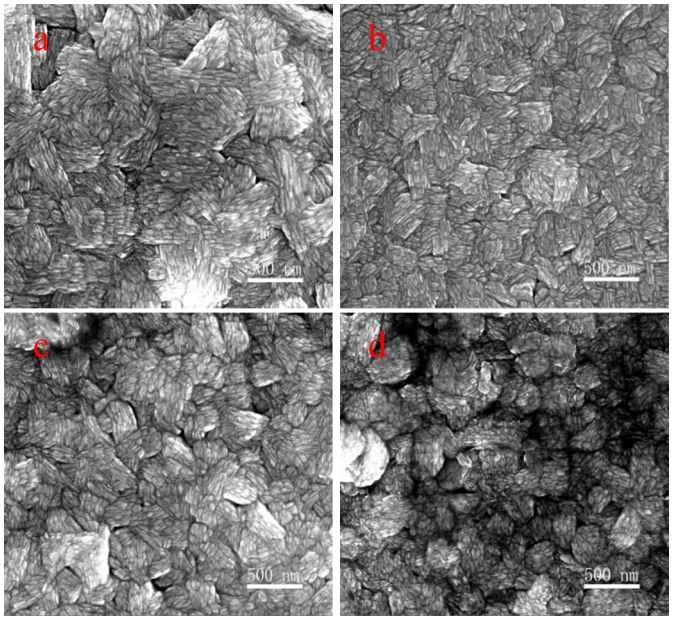

Fig. 2 FESEM morphology of zinc electrodeposited at J_f of 1 A/dm^2 from sulphate bath with different concentration of additive: (a) 0.5 g/L, (b) 1 g/L, (c) 1.5 g/L, and (d) 2 g/L.

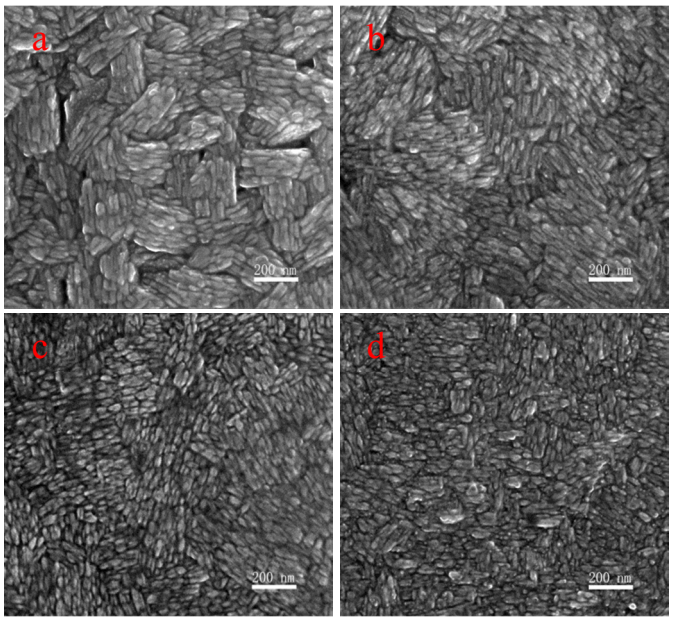

Fig. 3 FESEM morphology of zinc electrodeposited at different J_f from sulphate bath with additive (1 g/L): (a) 1 A/dm^2, (b) 2 A/dm^2, (c) 3 A/dm^2, and (d) 4 A/dm^2.

Effect of additive on grain size

Fig. 2 shows the influence of additives on the surface morphology of coatings. The additive is chosen according to Youssef's research,[2,28] in which nanocrystalline zinc coatings (56 nm) is electrodeposited by pulse current from zinc chloride electrolytes ($ZnCl_2$, NH_4Cl and H_3BO_3; pH=4.7) with polyacrylamide and thiourea as additives. The result shows that the PAM leads to a progressive reduction in grain size from a micro to a nano-scale (<100 nm), when compared with the coatings prepared from additive-free solution (Fig. 1). The results indicate that the PAM plays a primary role in grain refinement in this optimized sulfate bath. According to Youssef's research, the reduction of grain size by organic additives is mainly related to a combined effect of the increase of cathode overpotential, the retardation of continuous grain growth, the increase of nucleation of continuous grain growth and the increase of nucleation rate. The mechanism of the PAM is similar to the conventional zinc plating brightener, which suppresses the propagating of reagent particles and decreases the concentration of reactive ions, thereby increases the overpotential of cathode by organic additives absorption on the surface of electrode.[15] A relatively smoother and more uniform distribution of grain size is produced, when the concentration of PAM is 1 g/L, as shown in Fig. 2b. As PAM concentration increase continues, the coatings could relatively coarsen (as shown in Fig. 2c and Fig. 2d) and the PAM will precipitate out.

The influence of different J_f on the microstructure characteristics of coatings is examined in the range of 1 to 4A/dm^2, as shown in Fig. 3. The coatings, prepared from bath with PAM (1 g/L), are very homogeneous, dense and fine with approximately spherical-shaped particles. The grain size of coatings decreases gradually with increase of J_f from 1 to 3 A/dm^2. This trend can be explained by Sherik's theoretical:[29] increasing pulse current density can heighten overpotential which increases the free energy to form new nuclei and results in a higher nucleation rate and smaller grain size. Saber et al.[15] observed similar effects for nanocrystalline zinc electrodeposition in the chloride electrolytes system. They explained this trend and attributed the reduction of grain size to the high overpotential associated with the high pulse current density. At J_f=4 A/dm^2, the grain relatively coarsens, so the J_f should be controlled under 4 A/dm^2. The smallest grain size of the coatings is obtained at J_f of 3 A/cm^2, as seen from the image (Fig. 3c). FESEM studies also indicate that pulse current has an important action on grain size reduction in the presence of additive.

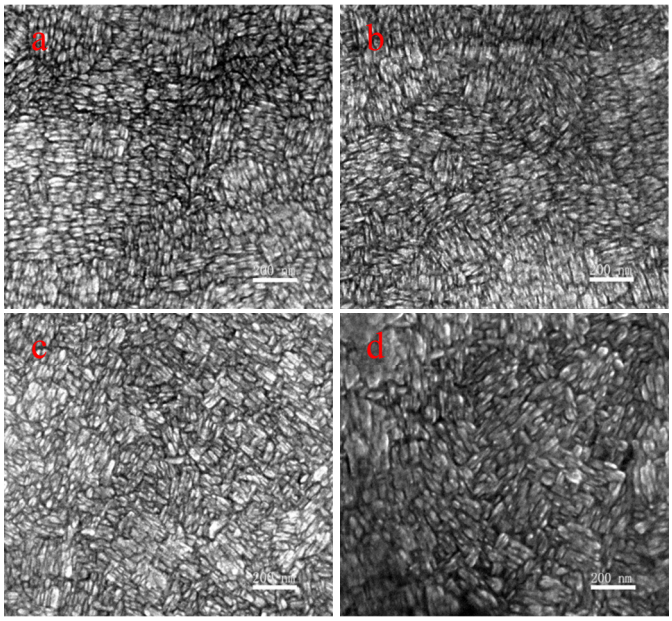

Fig. 4 FESEM images of zinc electrodeposited in the presence of pulse reverse current of (a) J_f=2 A/dm^2, J_r=0.2 A/dm^2, (b) J_f=3 A/dm^2, J_r=0.3 A/dm^2, (c) J_f=4 A/dm^2, J_r=0.4 A/dm^2, and (d) J_f=5 A/dm^2, J_r=0.5 A/dm^2 from sulfate-based electrolyte with additive (1 g/l).

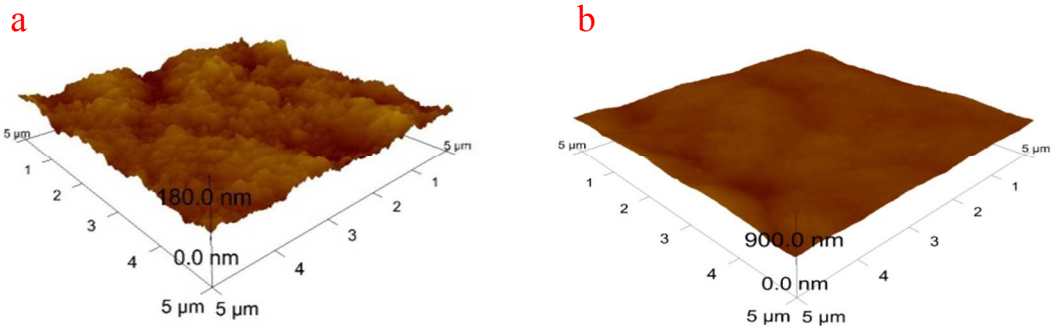

Fig. 5 AFM images of nanocrystalline zinc coatings obtained at (a) J_f=3 A/dm^2 and (b) J_f=3 A/dm^2, J_r=0.3 A/dm^2 from sulfate bath with additive (1 g/l).

Effect of pulse reverse current on grain size

The influences of pulse reverse currents on the surface morphology of coatings, are shown in Fig. 4 and Fig 5. These FESEM micrographs of the coatings are obtained from J_r of 0.2 A/dm^2 to 0.5 A/dm^2, respectively. As shown in Fig. 4, the pulse reverse current has not an obvious impact on the grain size of coatings with increasing J_r from 0.2 to 0.4 A/dm^2, when compared with the coatings produced at J_f of 3 A/dm^2 (Fig. 3c). Due to the addition of the pulse reverse current, the morphology of the coatings is more uniform and denser. Sequentially, increasing J_r from 0.4 to 0.5 A/dm^2 results in a progressive increase in the grain size of coating and the coating surface is relatively coarse and loose.

Surface morphology of coatings electrodeposited at different pulse reverse current densities is also studied by AFM measurement, as shown in Fig. 5. Through comparison, it is found that the surface of coatings obtained at J_r=0.3 A/dm^2 is smoother. Combination of SEM and AFM results suggests that the pulse reverse current does not have an obvious effect on

grain sizes, but achieves the effect of levelling off coatings while keeping J_f constant. The reason might be that reverse current dissolved those particles of larger grain size on the surface of coatings, and made the coatings smoother. An increase in J_f has the effect of decreasing the crystallite size, which has already been suggested in the preceding section. Other recent studies have investigated the viability of pulse current (The periodic pulse current with pulse only in positive direction.) in electrodeposition for better controlling the structure and properties of nanocrystlline zinc coatings and have obtained similar results.[30,31] The pulse reverse electrodeposition not only kept the advantages of pulse electrodeposition but also improved the performance of levelling off coatings, so the pulse reverse electrodeposition has a dual role in both smoothing and grain refinement of coatings than that of direct current electrodeposition. Besides, the anodic dissolution of reverse current makes the metal ion concentrations of cathode surface rise rapidly, which is favourable for using higher pulse current density in later cathode cycle. And the high pulse current density heightens the nucleation rate much more than the growth rate of coating, thus produces the coating with finer grain size.

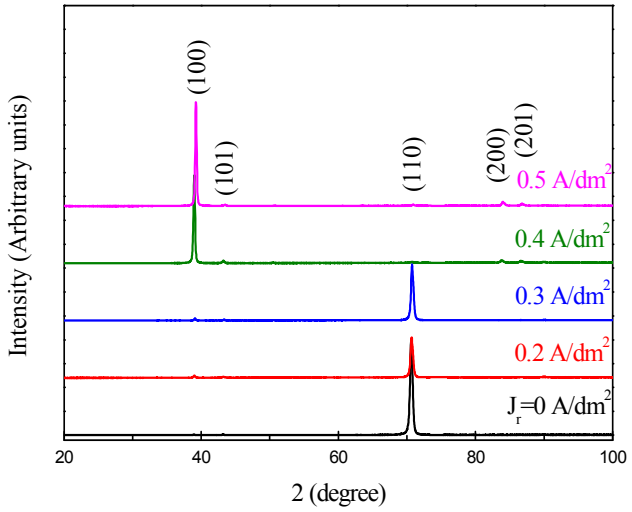

Fig. 6 XRD spectra of zinc electrodeposited at different Jr from sulfate-based electrolyte with additive (1 g/L).

The effects of increasing J_r on the preferred orientation and the grain size of coatings are shown in Fig. 6 and Fig. 7, respectively. Fig. 6 shows that the crystallographic orientation of coatings includes five obvious diffraction peaks of Zn (100), (101), (110), (200) and (201) associated with hexagonal structure. The diffraction peak intensity corresponding to the (110) plane is larger than other peaks, indicating that the deposits have well preferred orientation along (110) direction when the J_r increases from 0 to 0.3 A/dm^2. However, sequentially increasing J_r from 0.4 to 0.5 A/dm^2 alters the preferred orientation to the (100) crystal plane. The XRD analysis results indicated that the reverse current has significant influence on the crystallographic orientation. This is attributed to pulse current, which had a considerable effect on overpotential, thereby influenced the preferred orientation of coatings when the additive was present in bath, as reported in the literature.[22,28]

The average grain size of coatings calculated by Scherrer's formula,[32] at different J_r is shown in fig. 7. It can be inferred that the reverse current is not effective enough to reduce the grain size, but when increasing J_r from 0.4 to 0.5 A/dm^2, the largest grain size is produced. This trend is in good agreement with the surface morphology analysis results represented in Fig. 4.

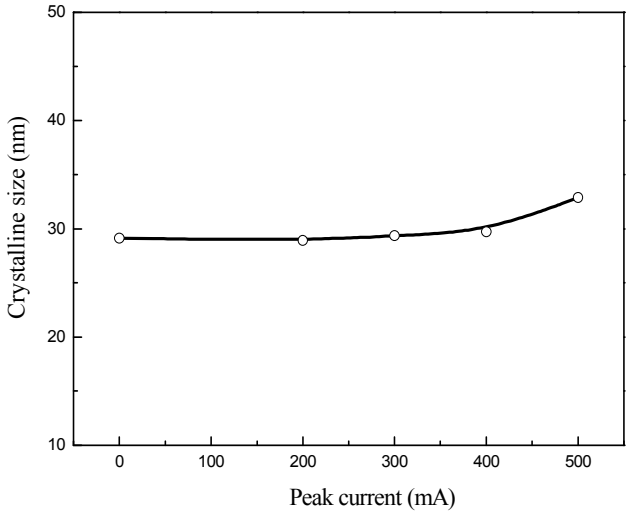

Fig. 7 Crystalline size of zinc electrodeposited at different Jr from sulfate-based electrolyte with additive (1 g/L).

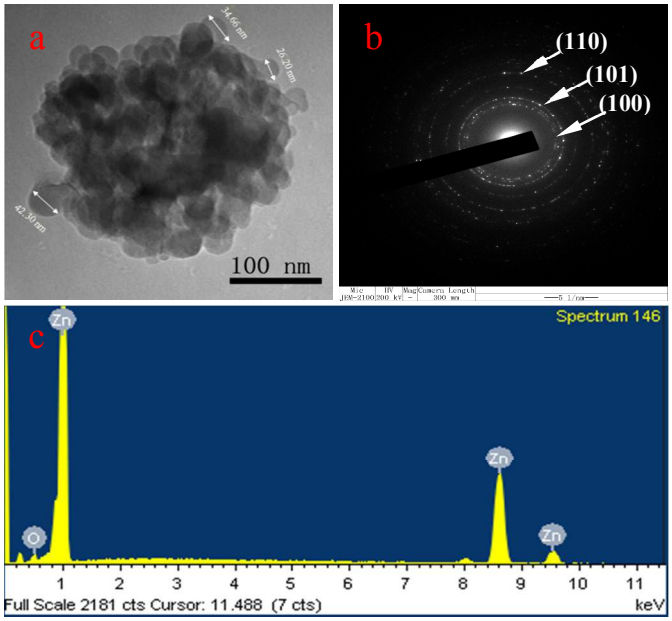

Fig. 8 TEM images and corresponding EDS spectra of zinc electrodeposition with J_f of 3 A/dm^2 and J_r of 0.3 A/dm^2 from sulfate-based electrolyte with additive (1 g/L): (a) TEM image of zinc electrodeposition, (b) Diffraction rings of zinc electrodeposited, and (c) EDS pattern for zinc electrodeposition.

Fig. 8 gives the TEM photomicrographs of coatings which are electrodeposited at J_f of 3 A/dm^2 and J_r of 0.3 A/dm^2 from a basic sulfate bath containing PAM of 1 g/L. Microstructure characterization by means of TEM observations indicates that the nonocrystalline zinc coating consists of ultrafine crystallites

in size range from 26 nm to about 42 nm, as shown in Fig. 8a. In presence of additive (PAM), the coating shows an approximately spherical-shaped structure and the average grain size is about 31 nm, which is a reasonable agreement with those observed results from the FESEM images and the average grain sizes obtained by the XRD technique. The corresponding selected-area electron diffraction (SAED) pattern can be indexed by the (100), (101), and (110) crystal planes of zinc, as shown in Fig. 8b. The nanocrystalline zinc coating also has been characterized by EDS (Fig. 8c), which shows that it is mainly composed by zinc. Detected oxygen is merely slight and its presence may be from the bath and the adsorption of oxygen in air. The EDS results also indicate that the nanocrystalline coating is pure zinc and not affected by oxidation after electrodeposition and before insertion into the TEM.

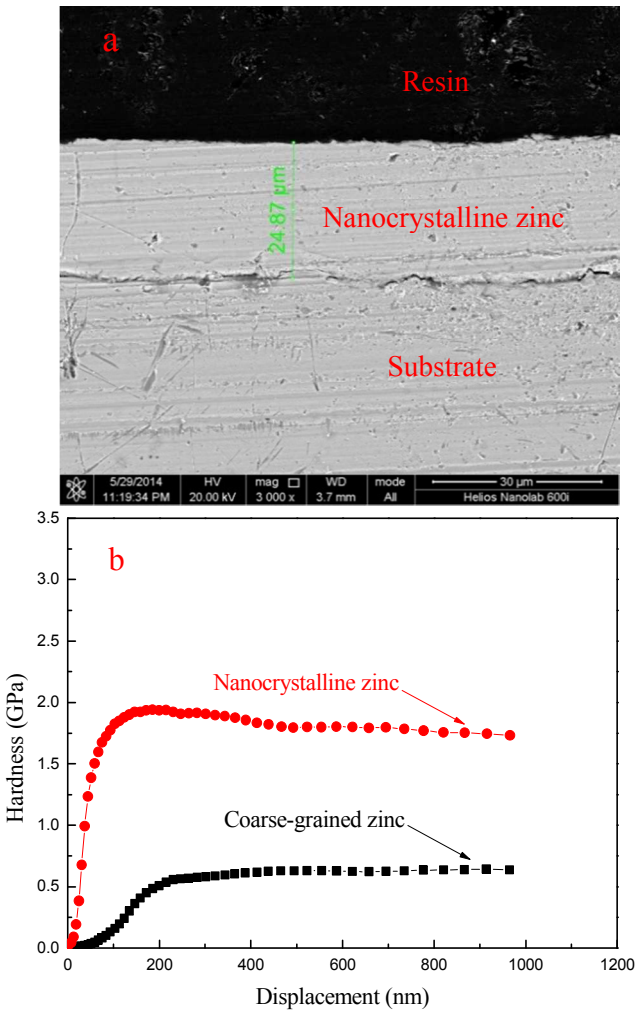

Fig. 9 Cross-section morphology (a) and hardness distribution (b) of nanocrystalline zinc coating.

Current efficiency of nanocrystalline zinc coating

The current efficiencies of coarse-grained (from the basic bath) and nanocrystalline (from the optimum bath) zinc coatings are measured by weight measurements, whose quantities are about 76% and 72% respectively. The difference between coarse-grained zinc and nanocrystalline zinc indicates that the additive decreases the current efficiency while refines the grain size of zinc coating. This result can be attributed to that the absorption of additive suppresses the propagating of reagent particles and decreases the concentration of reactive ions, thereby increases the overpotential of cathode (as stated above). The values of current efficiency are adequate to meet the requirements of the nanocrystalline zinc coatings production.

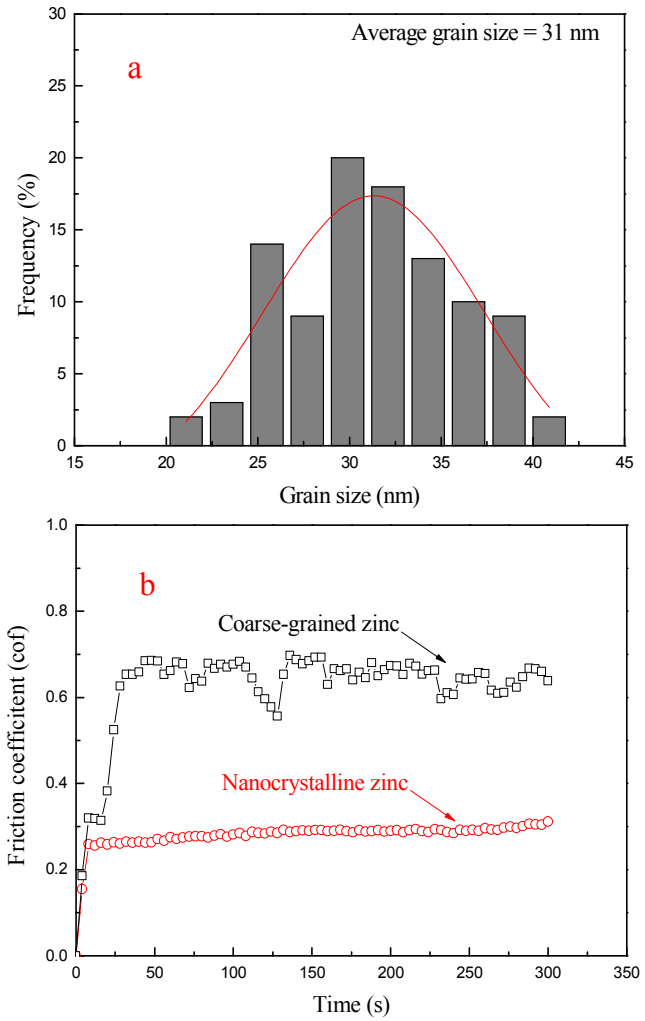

Fig. 10 Grain size distribution (a) and friction coefficients (b) of nanocrystalline zinc coating.

Mechanical performance of nanocrystalline zinc coating

Fig. 9 shows a cross-sectional morphology of the nanocrystalline zinc coating and hardness distribution along the thickness direction. Fig. 9a gives a cross-sectional observation of the nanocrystalline zinc coating which is obtained at J_f of 3 A/dm^2 and J_r of 0.3 A/dm^2 for 60min from the optimum bath. It can be seen that the nanocrystalline zinc coating with an average thickness of 24 μm has firm adherence to the substrate and almost no defects in the deposited regions. And the nanocrystalline zinc coating with a smooth surface has a uniform thickness distribution. The hardness-displacement curves through the thickness of coarse-grained and nanocrystalline zinc coatings, are shown in Fig. 9b. It can be seen that the hardness of the coarse-grained and nanocrystalline zinc coatings are 0.54 and 1.53 GPa, while the penetration

depth is 1000 nm. The hardness of nanocrystalline zinc coating is almost three times as that of coarse-grained zinc coating. This proves that the surface nanocrystallization of coating could enhance the hardness of coarse-grained zinc coating apparently.

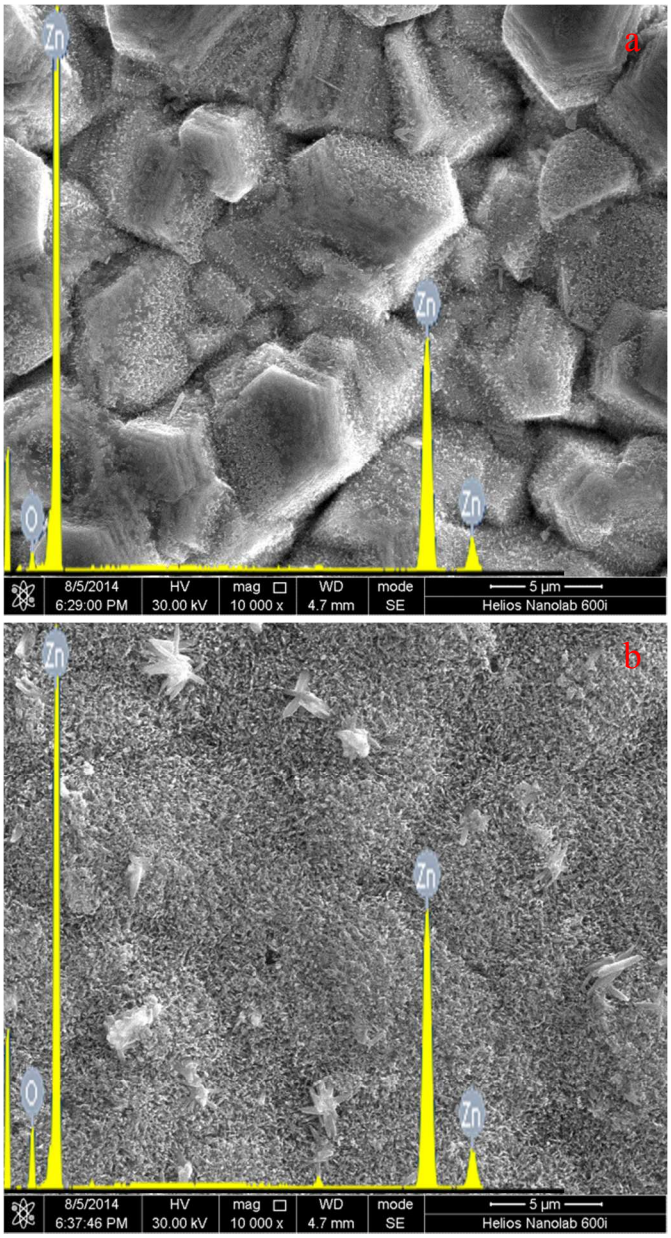

Fig. 11 FESEM morphologies and element compositions for corroded surfaces of coarse-grained (a) and nanocrystalline (b) zinc deposits after 100 h of immersion. The inset shows an EDS analysis of the surface.

Tribological property of nanocrystalline zinc coating

The grain size distribution of nanocrystalline zinc coating is determined from FESEM image by measuring more than 100 grains, as shown in Fig. 10a. The grains of the coating are highly dispersed with values ranging from 25 nm to 40 nm and the average grain size is 31 nm. Fig. 10b shows that the variation of the friction coefficients with the sliding duration for the coarse-grained and the nanocrystalline zinc coatings at an applied load of 1 N and a sliding speed of 0.188 m/s. It can be seen that the friction coefficients in both samples increase obviously in the initial period of sliding and tend to steady-state values. For the coarse-grained zinc coating, the friction coefficient varies in the range of 0.5-0.7 and the values are very unstable. Compared with the coarse-grained zinc coating, the friction coefficient of nanocrystalline zinc sample is between 0.2 and 0.3. The steady-state friction coefficients for the nanocrystalline zinc coating are obviously lower than that of the coarse-grained zinc coating. The differences between the coarse-grained and nanocrystalline zinc coatings approve that the surface nanocrystallization can decrease the friction coefficients of the deposit obviously. In general, under a certain load, the lower the friction coefficients, the better the wear resistance ability is.[33-35] Hence, it can be concluded that the nanocrystalline zinc coating exhibited excellent friction-reduction behavior and better wear resistance performance when compared with the coarse-grained zinc under the same wear conditions.

Corrosion resistance evaluation of nanocrystalline zinc coating

After 100 h of immersion in 3.5 % NaCl solution, FESEM observation is carried out for coarse-grained and nanocrystalline zinc coatings, as shown in Fig. 11. The images display that both surfaces are covered with corrosion product layers. In the case of coarse-grained zinc coating, the corrosion sites are discrete and local sites are corroded badly. It looks like that the coating is melted down. As for nanocrystalline zinc coating, the surface has been completely covered with a fine and uniform corrosion product layer, and has no abscission of coating because of the serious corrosion. The EDS spectrum of elemental composition of the coating surface shows that the deposits predominantly contain Zn and O. It is noteworthy that for both coatings in the same immersion times, the atomic oxygen content in the coarse-grained zinc coating is less than that of the nanocrystalline zinc coating. It can be deduced that the nanocrystalline zinc coating is more easily oxidative and form a dense and complete corrosion product layer during the immersion initial stage. According to the literature,[3,36] the corrosion product layers on both zinc coatings surface are mainly composed of ZnO, $Zn(OH)_2$ and $Zn_5(OH)_8Cl_2 \cdot H_2O$ (simonkolleite). In comparison with the coarse-grained zinc coating, the enhanced corrosion resistance of nanocrystalline zinc coating is mainly due to the better protection of the corrosion product layer. The nanocrystalline structure enhances both the kinetics of passivation and the stability of the passive film formed.[2] This can be explained that nanocrystalline materials are characterized by high-volume fraction of the grain boundary, so metal atoms that are at grain boundaries possess higher activity and are prone to corrosion. The volume fraction of the grain boundary is increased with the surface nanocrystallization of coating, thus the number of the surface activity sites is increased, which make the surface of nanocrystalline zinc coating rapidly form protective corrosion product film than the coarse-grained zinc coating.

Conclusions

Application of the pulse reverse current for nanocrystalline zinc electrodeposition from a sulfate bath containing PAM as the only additive resulted in more homogeneous, finer and denser distribution of grains, in comparison to those single pulse

electrodeposition samples. The following main findings resulted from the present investigation:

In additive-free electrolytes, no nanocrystalline zinc coating is obtained just through changing the pulse current density. The PAM can effectively reduce the grain size from micro to nano scale mainly due to the increases in the overpotential of cathode by absorption on the electrode surface. The grain size of nanocrystalline zinc coatings decreases gradually with increased pulse current density. The investigations also find that the pulse reverse current has the effect of altering the preferred orientation and levelling off coatings.

The pure nanocrystalline zinc coating with an average grain size of 31 nm and the (110) crystallographic preferred orientation is produced in this system under optimal conditions, and the thickness and surface grain size distribution are highly uniform. The hardness of the nanocrystalline zinc coating is almost three times as that of the coarse-grained zinc. The friction coefficient of the nanocrystalline zinc coating is much lower and more stable than that of coarse-grained zinc coating, which indicates that the nanocrystalline zinc coating exhibited excellent friction-reduction behaviour and better anti-wear performance.

The results of immersion test indicate that the nanocrystalline zinc coating shows much higher corrosion resistance than the coarse-grained zinc coating. The corrosion resistance property of nanocrystalline zinc coating is mainly due to the nanocrystalline structure which enhances both the kinetics of passivation and the stability of the formed passive film. Moreover, the current efficiency of nanocrystalline zinc coating is 72%, which is adequate to meet the requirements of the production. Therefore, the pulse reverse electrodeposition of nanocrystalline zinc coating is a quite effective method to improve properties of coarse-grained zinc coating.

Notes and references

[a] State Key Laboratory of Urban Water Resource and Environment, School of Chemical Engineering and Technology, Harbin Institute of Technology, No. 92 West-Da Zhi Street, Harbin 150001, China. Tel: 86-451-86418616; E-mail: mzan@hit.edu.cn.

1. P. Skarpelos and J.W. Morris Jr, *Wear*, 1997, **212**, 165.
2. K.M. Youssef, C.C. Koch and P.S. Fedkiw, *Corros. Sci.*, 2004, **46**, 51.
3. M.C. Li, L.L. Jiang, W.Q. Zhang, Y.H. Qian, S.Z. Luo and J.N. Shen, *J. Solid State Electrochem.*, 2007, **11**, 1319.
4. D.H. Jeong, F. Gonzalez, G. Palumbo, K.T. Aust and U. Erb, *Scripta Mater.*, 2001, **44**, 493.
5. S. Tao and D. Li, *Nanotechnology*, 2006, **17**, 65.
6. Y.R. Jeng, P.C. Tsai and S.H. Chiang, *Wear*, 2013, **303**, 262.
7. M.S. Chandrasekar and P. Malathy, *Mater. Chem. Phys.*, 2010, **124**, 516.
8. F. Nasirpouri, M.R. Sanaeian, A.S. Samardak, E.V. Sukovatitsina, A.V. Ognev, L.A. Chebotkevich, M.-G. Hosseini and M. Abdolmaleki, *Appl. Surf. Sci.*, 2014, **292**, 795.
9. L. Lu, M.L. Sui and K. Lu, *Science*, 2000, **287**, 1463.
10. L. Lu, X. Chen, X. Huang and K. Lu, *Science*, 2009, **323**, 607.
11. M. Hakamada, Y. Nakamoto, H. Matsumoto, H. Iwasakib, Y. Chena, H. Kusudaa and M. Mabuchi, *Mater. Sci. Eng. A*, 2007, **457**, 120.
12. X. Yuan, Y. Wang, D. Sun and H. Yu, *Surf. Coat. Technol.*, 2008, **202**, 1895.
13. L. Lu, Y. Shen, X. Chen, L. Qian and K. Lu, *Science*, 2004, **304**, 422.
14. R. Ramanauskas, L. Gudavičiūtė, R. Juškėnas and O. Ščit, *Electrochim. Acta,* 2007, **53**, 1801.
15. K. Saber, C.C. Koch and P.S. Fedkiw, *Mater. Sci. Eng. A*, 2003, **341**, 174.
16. H.B. Muralidhara and Y. Arthoba Naik, *Surf. Coat. Technol.*, 2008, **202**, 3403.
17. B.H. Juárez and C. Alonso, *J. Appl. Electrochem.*, 2006, **36**, 499.
18. G. Meng, L. Zhang, Y. Shao, T. Zhang and F. Wang, *Corros. Sci.*, 2009, **51**, 1685.
19. H. Yan, J. Downes, P.J. Boden and S.J. Harris, *J. Electrochem. Soc.*, 1996, **143**, 1577.
20. M.C. Li, L.L. Jiang, W.Q. Zhang, Y.H. Qian, S.Z. Luo and J.N. Shen, *J. Solid State Electrochem.*, 2007, **11**, 549.
21. A. Gomes and M.I. da Silva Pereira, *Electrochim. Acta*, 2006, **51**, 1342.
22. K.M. Youssef, C.C. Koch and P.S. Fedkiw. *Electrochim. Acta*, 2008, **54**, 677.
23. L. Chang, *J. Alloys Compd.*, 2008, **466**, L19.
24. K.M. Yin, *Surf. Coat. Technol.*, 1997, **88**, 162.
25. N.V. Mandich, *Met. Finish.*, 2000, **98**, 375.
26. M.S. Chandrasekar and M. Pushpavanam, *Electrochim. Acta*, 2008, **53**, 3313.
27. W. Cheng, W. Ge, Q. Yang and X.X. Qu, *Appl. Surf. Sci.*, 2013, **276**, 604.
28. K.M. Youssef, C.C. Koch and P.S. Fedkiw, J. Electrochem. Soc., 2004, **151**, C103.
29. A.M. El-Sherik and U. Erb, *J. Mater. Sci.*, 1995, **30**, 5743.
30. M.S. Chandrasekar and P. Malathy, *Mater. Chem. Phys.*, 2010, **124**, 516.
31. M.S. Chandrasekar, S. Srinivasan and M. Pushpavanam, *J. Mater. Sci.*, 2010, **45**, 1160.
32. B.D. Cullity, *Elements of X-ray Diffraction, second ed., Addison Wesley Publishing Company, Inc., Philippines,* 1978, p. 284.
33. X.L. Lei, B. Shen, S.L. Chen, L. Wang and F.H. Sun, *Tribol. Int.*, 2014, **69**, 118.
34. A.K. Pradhan and S. Das, *Tribol. Trans.*, 2014, **57**, 46.
35. K.H. Hou, H.H. Sheu and M.D. Ger, *Appl. Surf. Sci.*, 2014, **308**, 372.
36. D. de la Fuente, J.G. Castano and M. Morcillo, *Corros. Sci.*, 2007, **49**, 1420.

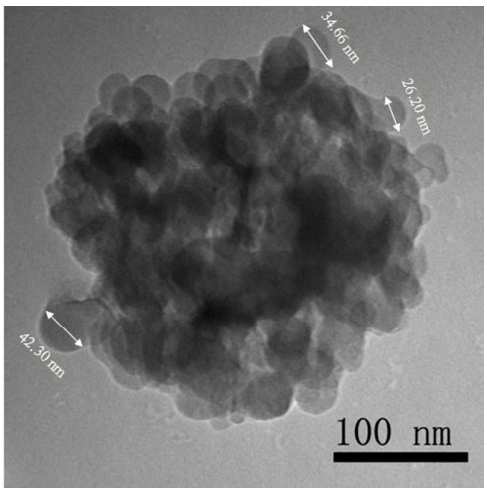

The nanocrystalline zinc coating is produced by pulse reverse electrodeposition in sulfate bath with polyacrylamide as the only additive. Mechanical, wear and corrosion resistance properties of nanocrystalline and coarse-grained zinc coatings are evaluated by nanoindentation, ball-on-disc tribometer and immersion test, respectively.